Unified Framework for Ionization Balance and Equation of State in Partially Ionized Plasmas from Structure Factors

Chengliang Lin(林成亮)[1], Yong Hou(侯永)[2*], Jianmin Yuan(袁建民)[2,3*], Yong Wu(吴勇)[1*], and Jianguo Wang(王建国)[1]

[1]*National Key Laboratory of Computational Physics, Institute of Applied Physics and Computational Mathematics, Beijing 100088, China*

[2]*College of Science, National University of Defense Technology, Changsha 410073, China*

[3]*Institute of Atomic and Molecular Physics, Jilin University, Changchun 130012, China*

(Received 11 February 2026; accepted manuscript online 30 March 2026)

The ionization balance and charge state distribution of partially ionized plasmas are fundamental to predicting the key properties like the equation of state and transport properties. However, its determination remains contentious because of the ambiguous partitioning of electronic states into free and bound components. Here, we present a unified framework that rigorously connects the ionization potential depression, the ionization degree, and the equation of state through the structure factors. By incorporating thermal kinetic bottlenecks and pressure ionization via a modified partition function, and treating ionization potential depression through structure factors, the model resolves longstanding discrepancies in predicted ionization degrees. It accurately reproduces path integral Monte Carlo equations of state of hydrogen plasmas across a broad range of densities and temperatures, clarifies the competing roles of thermal and pressure ionization, and provides a clear link between microscopic electronic structure and macroscopic thermodynamics. This work offers a predictive and thermodynamically consistent foundation for modeling partially ionized plasmas in high energy density and astrophysical contexts.

DOI: 10.1088/0256-307X/43/5/050302 CSTR: 32039.14.0256-307X.43.5.050302

Dense partially ionized plasma is ubiquitous in astrophysical objects from dwarf stars to planetary interiors,[1–3] and is routinely produced in laboratory experiments in inertial confinement fusion[4–6] and high-energy-density physics.[7,8] Its description must simultaneously account for strong Coulomb coupling, partial electron degeneracy, thermal excitation, and partial ionization. A central and particularly elusive aspect is the electronic structure and the associated charge-state distribution, which underlies key plasma properties such as the equation of state (EOS),[9–12] opacity,[13,14] and transport coefficients.[15–17] However, determining ionization in dense plasmas remains contentious, hampered by the lack of a unique quantum-mechanical definition[18–20] and by the ambiguous partitioning of electrons into bound and free states.[21–25]

The ambiguity in bound-free partitioning leads to stark discrepancies across theoretical approaches. While simulation methods, such as path integral Monte Carlo (PIMC)[26–29] and molecular dynamics,[30–33] treat electron-ion correlations without *a priori* assumptions about ionization states, they struggle to extract unambiguous ionization signatures. Consequently, the extraction criteria or external approximations imposed *a posteriori* lead to significant discrepancies in the ionization degree[26,27,34,35] and even to contradictory conclusions regarding phenomena like the plasma-phase transition in hydrogen.[20,36,37] Hence, a self-consistent route to simultaneously determine the thermodynamical properties and ionization degree is highly demanded. Conversely, chemical picture models, based on a partition of electronic states into bound and continuum components, rely on an inherently ambiguous separation due to the same Coulomb interaction that both binds atoms and dissolves them in the plasma environment. In dense plasmas, two phenomena become essential within such chemical descriptions: ionization potential depression (IPD) and renormalization of atomic partition function (PF). IPD quantifies the downward shift of the continuum edge due to plasma effects, effectively lowering the ionization energy.[38–42] PF characterizes the statistical sum over all thermally accessible bound states at a given temperature, which diverges for an isolated atom because of the infinite series of Rydberg states. In plasmas, this divergence is regularized into a finite value due to environmental interactions.[43–47] Both IPD and PF are manifestations of the same underlying Coulomb many-body environment and jointly define the bound-free partitioning. Consequently, predictions of ionization balance and thermodynamics are highly sensitive to the specific models adopted for IPD and the renormalized PF. These inconsistencies underscore the urgent need for a unified framework that rigorously links ionization to measurable structural and thermodynamic properties.

To resolve these longstanding challenges, we focus

*Corresponding authors. Email: yonghou@nudt.edu.cn; yuanjianmin@jlu.edu.cn; wu_yong@iapcm.ac.cn

© 2026 Chinese Physical Society and IOP Publishing Ltd. All rights, including for text and data mining, AI training, and similar technologies, are reserved.

on the simplest hydrogen plasma system. Its seemingly straightforward composition of protons and electrons belies a rich complexity, featuring phenomena such as the formation of atoms and molecules, dissolution of bound states (Mott effect), and a nontrivial EOS.[37] These characteristics make hydrogen an indispensable benchmark for theoretical models. However, recent first-principles simulations have revealed contradictory predictions regarding the ionization balance[26,27] and magnitude of the IPD,[34,35] highlighting persistent gaps in our fundamental understanding. Resolving these issues in hydrogen not only clarifies the physics of a prototypical Coulomb system but also establishes a critical foundation for modeling more complex, multicomponent plasmas.

In this Letter, we develop a unified theoretical framework that rigorously connects ionization balance to the structure factors (SFs) of plasmas. Our model self-consistently determines the IPD, the average ionization degree, and the EOS. Applying this unified framework to warm dense hydrogen plasmas, it reconciles discrepancies between existing methods, accurately reproduces high-fidelity EOS data of PIMC,[26,27] and provides a clear microscopic interpretation of electronic structure and macroscopic thermodynamics in partially ionized plasmas, offering a predictive tool for both fundamental studies and applied high-energy-density research.

In the chemical picture, ionization equilibrium in plasmas is governed by a generalized Saha equation. It can be derived from a statistical decomposition of the electronic density of state (DOS) and the subsequent minimization of the system's free energy.[21,22] A fundamental difficulty in this approach arises because the boundary between bound and continuum states is not sharply defined but represents a continuous statistical transition.[48,49] Assigning an electronic state as bound or free essentially distributes portions of the interaction energy into the effective PF and the IPD,[50] so that they are not independent but must be interrelated through comprehensive thermodynamic self-consistency.[51] The influence of many-body interactions among charged particles on electronic states is inherently dynamic. Effects such as dynamic screening, collisions, and thermal fluctuations modify the lifetime and energy distribution of bound states, leading to level broadening, shifts, and mixing. The IPD mainly represents the time-averaged correction to the ionization energy, which is defined as the relative difference of ground state energy of a bound system and the one of its ionized partner. Other non-ideal plasma effects, such as fluctuations and dynamic collisions, can be incorporated by modifying the statistical weights in the PF. Together, the IPD and PF provide a complementary description of dynamic response and statistical fluctuation of plasmas. For hydrogen plasmas, the resulting Saha equation takes the form[45,52]

$$\frac{n_{\mathrm{H}}}{n_{\mathrm{p}}^{*}} = u_{\mathrm{H}} \exp(\beta I_1 - \beta \Delta_{\mathrm{IPD}} + \beta \mu_{\mathrm{e}}^{\mathrm{id}}), \tag{1}$$

where n_{H} and n_{p}^{*} are the densities of neutral hydrogen atoms and protons, respectively. The unperturbed ionization energy of level n is $I_n = E_{\mathrm{ryd}}/n^2$, with the Rydberg energy $E_{\mathrm{ryd}} = e^2/(8\pi\epsilon_0 a_{\mathrm{B}})$ and the Bohr radius a_{B}. Here, Δ_{IPD} denotes the IPD, and $\beta = 1/(k_{\mathrm{B}}T)$ is the inverse temperature. $\mu_{\mathrm{e}}^{\mathrm{id}}$ represents the chemical potential of an ideal Fermi gas with density $n_{\mathrm{e}}^{*} = n_{\mathrm{p}}^{*}$, given by[45]

$$n_{\mathrm{e}}^{*} = \frac{2}{\lambda_{\mathrm{e}}^{3}} F_{1/2}(\beta \mu_{\mathrm{e}}^{\mathrm{id}}), \tag{2}$$

where $\lambda_{\mathrm{e}} = \sqrt{2\pi\hbar^2\beta/m_{\mathrm{e}}}$ is the electron thermal wavelength and $F_\nu(x) = \frac{1}{\Gamma(\nu+1)} \int_0^\infty \mathrm{d}t \frac{t^\nu}{\mathrm{e}^{t-x}+1}$ is the Fermi integral of order ν with the Gamma function $\Gamma(\nu)$.

The atomic PF u_{H} in Eq. (1) generally incorporates a weighting factor ω_n that accounts for plasma-induced truncation of bound states,[22,44,53] and reads

$$u_{\mathrm{H}} = \sum_{n=1}^{\infty} 2n^2 \, \omega_n \, \mathrm{e}^{-\beta\varepsilon_n}, \tag{3}$$

where $\varepsilon_n = I_1(1 - 1/n^2)$ is the excitation energy of state n with respect to the ground state. The choice of ω_n is not unique and represents a central challenge in the modeling of dense plasmas. Different models for ω_n correspond to different physical interpretations of how the bound states merge into the continuum. The IPD-based truncation model $\omega_n^{\mathrm{IPD}} = H(I_n - \Delta_{\mathrm{IPD}})$ with the Heaviside function $H(x)$ is often applied, which may lead to unphysical discontinuities in thermodynamic quantities.[47,52,54] In plasmas, weakly bound states are destabilized by thermal collisions, with their diffuse wavefunctions blurring into the continuum. Simultaneously, low-energy electrons can be transiently trapped in multi-ion potentials, preventing them from being regarded as truly free. This fundamental ambiguity calls for a smooth weighting factor ω_n to physically partition their contributions to the PF, such as the microfield model introduced by Hummer and Mihalas (HM).[43] It achieves smoothness through a cumulative microfield distribution, but may lack statistical consistency.[47] Another widely used weighting factor in EOS calculations is the Planck–Brillouin–Larkin (PBL) form $\omega_n^{\mathrm{PBL}} = 1 - \mathrm{e}^{-\beta I_n} - \beta I_n \mathrm{e}^{-\beta I_n}$,[55,56] which characterizes the physical fact that electronic states with binding energies less than $k_{\mathrm{B}}T$ are not stable with respect to dynamic collisions and thermal fluctuations. However, ω_n^{PBL} does not account for density-dependent effects on PF and thus cannot describe the pressure ionization of bound states. Following More's treatment for pressure ionization,[57,58] we propose a modified PBL form

$$\omega_n^{\mathrm{mPBL}} = \frac{\omega_n^{\mathrm{PBL}}}{1 + [a \, E_{\mathrm{ryd}}/(I_n r_{\mathrm{WS}})]^b}, \tag{4}$$

with $r_{\mathrm{WS}} = [4\pi(n_{\mathrm{H}} + n_{\mathrm{p}}^{*})a_{\mathrm{B}}^3/3]^{-1/3}$, which ensures both a smooth truncation of PF and a transparent manifestation of pressure ionization and thermal fluctuations. In this work, the specific values of $a = 3$ and $b = 4$ are adopted.[58,59] These values were determined by fitting the average ionization state calculated using More's model for pressure ionization to the corresponding results from Thomas–Fermi calculations.[59]

The second key quantity in Eq. (1) is the IPD. We adopt the SF-based model derived from the Green's

function approach. In this model, many-body effects are encoded in the dielectric function, which is connected to the dynamical SF via the fluctuation-dissipation theorem.[52,60] Following Chihara's treatment,[61,62] the dynamical SF can be decomposed into two parts, a contribution from fast-moving free electrons, and an ionic part that includes the screening cloud of the slowly moving electrons following the ionic motion. The IPD for hydrogen is obtained by averaging over the frequency of dynamical SF,

$$\Delta_{\rm IPD}=\frac{2E_{\rm ryd}\kappa_{\rm eff}^2}{\pi\, r_{\rm S}}\int_0^\infty\frac{{\rm d}q}{q^2}\left\{S_{\rm ee}^0(q)+[1-f_{\rm scr}(q)]^2S_{\rm pp}(q)\right\}. \quad (5)$$

Here, $r_{\rm S}=a_{\rm ee}^*/a_{\rm B}$ with the average distance of free electrons $a_{\rm ee}^*=(4\pi n_{\rm e}^*/3)^{-1/3}$, q is the wavenumber in units of $1/a_{\rm ee}^*$, and $\kappa_{\rm eff}^2=3\Gamma_{\rm ee}^*/\sqrt{1-0.4(3\gamma_0^2\Gamma_{\rm ee}^*)^{3/4}+3\gamma_0^2\Gamma_{\rm ee}^*}$ with $\gamma_0=(9\pi/4)^{-1/3}$ and the coupling parameter $\Gamma_{\rm ee}^*=2\mathcal{R}\beta/r_{\rm S}$. The contribution of rapidly moving free electrons is accounted for by the SF of the interacting electron gas $S_{\rm ee}^0(q)$. The screening cloud formed by slower-moving electrons around protons is described by $f_{\rm scr}(q)$, which is connected to $S_{\rm ee}^0(q)$.[62] Meanwhile, $S_{\rm pp}(q)$ corresponds to the static SF of protons in hydrogen plasmas.

For partially ionized hydrogen plasmas, the total pressure must account for contributions from all interparticle interactions. In the parameter range studied here, charge-neutral and neutral-neutral interactions have a negligible effect on EOS and are omitted.[27] The total pressure of hydrogen plasmas is thus given by

$$P=P_{\rm H}+P_{\rm p}+P_{\rm e}+P_{\rm coul}, \quad (6)$$

where $P_{\rm e}=2F_{3/2}(\beta\mu_{\rm e}^{\rm id})/\beta\lambda_{\rm e}^3$ is the ideal Fermi-gas pressure, $P_{\rm H}=n_{\rm H}k_{\rm B}T$ and $P_{\rm p}=n_{\rm p}^*k_{\rm B}T$ are the classical ideal-gas contributions of atoms and protons, respectively. $P_{\rm coul}$ denotes the excess pressure from Coulomb interactions $v_{ab}(r)=z_az_be^2/(4\pi\epsilon_0 r)$, which is evaluated using the virial formula[45]

$$\beta P_{\rm coul}=-\frac{2\pi}{3k_{\rm B}T}\sum_{a,b={\rm e,p}}n_a^*n_b^*\int_0^\infty g_{ab}(r)\frac{{\rm d}v_{ab}(r)}{{\rm d}r}r^3{\rm d}r. \quad (7)$$

Performing Fourier transforms of the radial distribution functions $g_{ab}(r)$, and applying the Chihara decomposition to the SFs consistent with our IPD treatment, yields

$$\beta P_{\rm coul}=\frac{n_{\rm e}^*\Gamma^*}{3\pi}\int_0^\infty{\rm d}q\left\{S_{\rm ee}^0(q)+[1-f_{\rm scr}(q)]^2S_{\rm pp}(q)-2\right\}. \quad (8)$$

The above formulations constitute a unified functional framework that self-consistently determines the ionization degree and EOS of partially ionized hydrogen plasmas through static SFs. This approach ensures thermodynamic consistency between the IPD, the PF, and the EOS, which can be straightforwardly generalized to multi-component plasmas. In the following, we apply it to investigate the ionization balance and EOS in warm dense hydrogen, validating the model against high-fidelity PIMC simulations. In following calculations, the proton SF $S_{\rm pp}(q)$ is derived from a reference one-component charged hard-sphere system,[62] treated within the mean spherical approximation.[63,64] Within this framework, the screening function $f_{\rm scr}(q)$ is also determined.[62,65] The free-electron SF $S_{\rm ee}^0(q)$ is evaluated using an analytical model proposed in Ref. [66].

We begin by analyzing the bound-free partitioning of electronic DOS underlying the derivation of Saha Eq. (1).[21,22] In the conventional Saha picture, the free-electron DOS is $g_{\rm F}(E)=2r_{\rm S}^2\sqrt{\bar{\varepsilon}}/(3\pi)$ with $\bar{\varepsilon}=E/E_{\rm ryd}$,[48] while the bound-state DOS is represented by a sum of delta functions $\sum_n 2n^2\delta(E+I_n)$.[21] To better capture the continuous nature of electronic states, we adopt a classical atomic DOS for hydrogen $g_{\rm H}(E)=(-\bar{\varepsilon})^{-5/2}$.[48,49] As shown in Fig. 1(a), $g_{\rm H}(E)$ and $g_{\rm F}(E)$ are discontinuous at $E=0$, leading to a divergent atomic PF that requires renormalization. A simple renormalization scheme incorporates the IPD effect to shift the bound-state continuum downward. The corresponding DOS for $r_{\rm WS}=20$ and $T=62500\,{\rm K}$ is plotted in Fig. 1(a). Although this scheme truncates bound-state contributions with principal quantum numbers $n>4$, rendering the PF $u_{\rm H}$ finite, a discontinuous jump between free and bound DOS persists. This discontinuity ultimately produces the abrupt change in predicted ionization degree seen in Fig. 1(e). Figure 1(b) presents a continuously varying electronic DOS, alongside the bound-state contributions included in $u_{\rm H}$ under different cutoff schemes for the weight factor ω_n. These schemes yield markedly different effective bound-state energy ranges, leading to substantial variations in the predicted ionization degree. This inherent uncertainty propagates into other thermodynamic properties, such as the EOS.

Figure 1(c) displays the weight factor ω_n versus the principal quantum number n for different models. Compared to the HM model[43] and IPD model $\omega_n^{\rm IPD}$, both the PBL and mPBL models exhibit significant suppression even from $n=1$, a feature attributable to thermal collisions in the plasma. In cold neutral plasmas, states with $n\gtrsim\sqrt{\beta E_{\rm ryd}}$ cannot form stable bound states via three-body recombination due to a kinetic bottleneck:[67] electrons recombining into these states are highly susceptible to immediate reionization through subsequent collisions with nearby ions and electrons, preventing significant population buildup and formation of stable bound states. This bottleneck is effectively incorporated in the PBL-type PFs, which suppresses contributions from states with $n\gtrsim\sqrt{\beta E_{\rm ryd}}$, preventing their interpretation as strictly bound.

The PFs and corresponding ionization degrees are compared across models as functions of density in Figs. 1(d) and 1(e). At low densities, PFs from PBL-type models are substantially lower than those from the HM[43] and IPD models, reflecting the kinetic bottleneck effect. With increasing density and coupling strength, density effects dominate and pressure-driven ionization becomes significant. In this regime, our mPBL model (4) converges toward the trend predicted by the HM model. In the intermediate regime ($\Gamma\sim1$), a nontrivial competition between thermal and density effects emerges. Generally, a smaller PF corresponds to fewer bound states and thus a higher ionization degree.

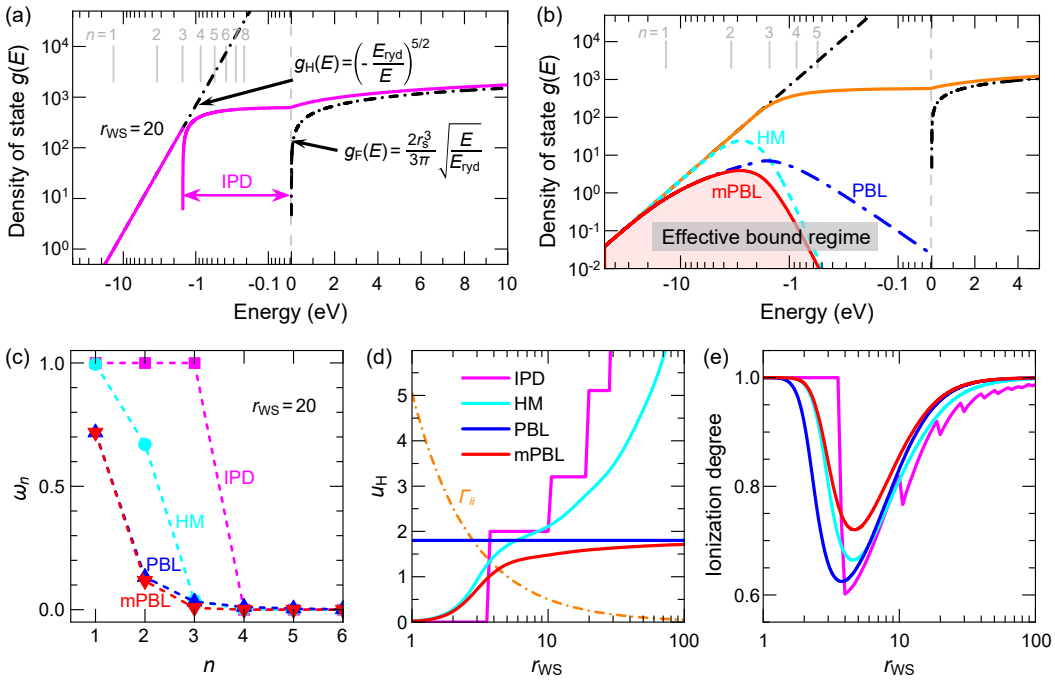

Fig. 1. Density and temperature effects on the electronic structure and ionization balance of the hydrogen plasmas at $T = 62500\,\mathrm{K}$. (a) DOS at $r_{\mathrm{WS}} = 20$ for the unperturbed case (dash-dotted black curves) and with the IPD effect (magenta lines), which corresponds to the truncation model with ω_n^{IPD}. (b) The effective bound regime $w_n\, g(E)$ at $r_{\mathrm{WS}} = 20$ predicted by the HM, PBL (ω_n^{PBL}), and mPBL (ω_n^{mPBL}) model, respectively. The solid orange line represents the electronic DOS $g(E)$. (c) The effective cutoff in the PF at $r_{\mathrm{WS}} = 20$ for different principle quantum number n in the IPD[44,52] (magenta squares), HM[43] (cyan circles), PBL[55,56] (ω_n^{PBL}, blue upper triangles), and mPBL (ω_n^{mPBL}, red lower triangles) model, respectively. The lines are guides to the eyes. (d) and (e) Density dependence of the PF and the corresponding ionization degree calculated with the IPD (ω_n^{IPD}, magenta), HM (cyan), PBL (ω_n^{PBL}, blue), and mPBL (ω_n^{mPBL}, red) model, respectively.

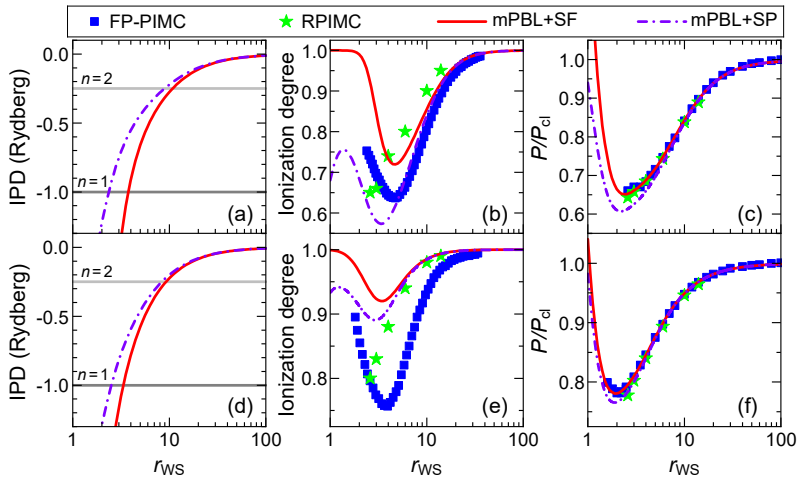

Fig. 2. Density dependence of the IPD, the ionization degree, and the pressure of hydrogen plasmas at $T = 62500\,\mathrm{K}$ [(a), (b), (c)] and $T = 125000\,\mathrm{K}$ [(d), (e), (f)]. The influence of different IPD models on the ionization degree and the pressure are depicted by the red solid curves [mPBL+SF for ω_n^{mPBL} (4) with SF IPD model (5)] and the violet dash-dotted curves [mPBL+SP for ω_n^{mPBL} (4) with SP IPD model[38]]. For comparison, the simulation data for the pressure and the extracted ionization degree from the fermionic propagator PIMC[27] (FP-PIMC, blue squares) and the restricted PIMC[26] (RPIMC, green stars) method are also presented.

To elucidate plasma effects on ionization energy, we compare the widely used Stewart-Pyatt (SP) IPD model[38] with our SF model (5). The SP model is commonly employed in astrophysical modeling. Figures 2(a) and 2(d) show the IPD as a function of density for $T = 62500\,\mathrm{K}$ and $T = 125000\,\mathrm{K}$, respectively. At low density, both models converge to the Debye–Hückel limit.[45] However, as the coupling strength increases, the SP model increasingly underestimates the IPD due to its incomplete treatment of strong-coupling effects. Consequently, the SP model predicts a lower ionization degree than the SF model, as shown in Figs. 2(b) and 2(e). In contrast, the

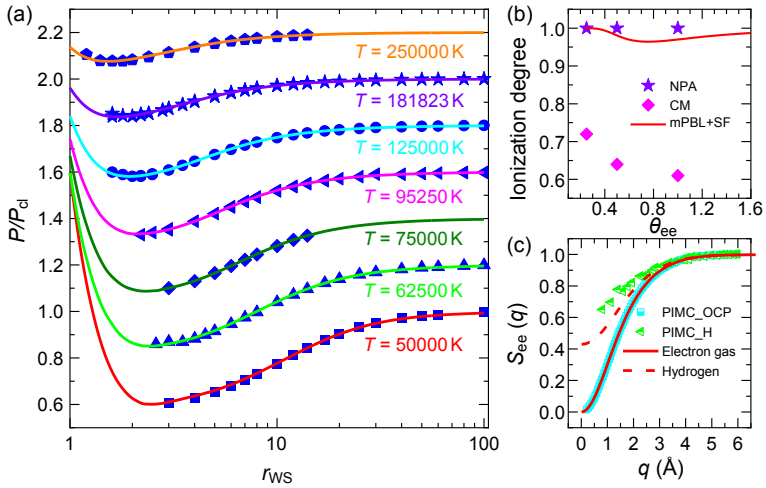

Fig. 3. (a) Comparison of the pressure calculated with mPBL+SF model (solid lines) with FP-PIMC simulation data[27] (symbols) for hydrogen plasmas under a wide range of densities and temperatures. As the temperature increases, the pressure data corresponding to different temperatures shift upward sequentially with an interval of 0.2. (b) The ionization degree at $r_{\rm WS} = 2$ with different temperatures (i.e. different electron degeneracy cases). For comparison, the predictions from the NPA[19,68] (violet stars) and CM[29,35] (magenta diamonds) models at electron degeneracy $\theta_{\rm ee} = 0.25$, 0.5, 1 are also shown. (c) Comparison of the calculated structure factor for electron gas (OCP) and the hydrogen plasma at $r_{\rm WS} = 2$ and $\theta_{\rm ee} = 1$ with the PIMC simulation data[28] for the uniform electron gas system and for the hydrogen plasma.

SF model inherently incorporates many-body correlations through the static SF, which naturally captures the enhanced suppression of the ionization energy with stronger coupling. At very high densities ($r_{\rm WS} \sim 1.5$), the SP model yields an unphysical weakening of pressure ionization. For $T = 62500$ K, the onset density for significant pressure ionization in the SF model aligns closely with PIMC results,[26,27] whereas the SP model requires a higher density to exhibit comparable pressure-driven ionization. This discrepancy leads to a lower pressure prediction from the SP model compared to the SF model in Fig. 2(c). Notably, the pressure derived from our SF model shows excellent agreement with PIMC data.[26,27] Similar trends for ionization degree and EOS are observed at $T = 125000$ K [Figs. 2(d)–2(f)], although the higher ionization at this temperature reduces the EOS discrepancy between the two models.

A comparison of ionization degrees in Figs. 2(b) and 2(e) reveals substantial discrepancies among values extracted using different PIMC-based methods,[26,27] while the corresponding pressures remain remarkably consistent, as displayed in Figs. 2(c) and 2(f). This inconsistency underscores the urgent need for a unified theoretical framework that can simultaneously describe different physical quantities. While high-fidelity simulations like PIMC provide reliable thermodynamic data and structural details, the inferred ionization degree remains sensitive to the specific extraction protocol applied. Our theoretical framework addresses this challenge by offering a self-consistent route to simultaneously determine the SF, EOS, and ionization degree.

To further validate our model, we perform a comprehensive comparison of the hydrogen EOS over a wide range of temperatures and densities, as shown in Fig. 3(a). The agreement is excellent throughout, confirming the broad applicability of our approach. A notable inflection in the pressure ratio $P/P_{\rm cl}$ occurs near $r_{\rm WS} = 2$, which approximately marks the onset of pressure ionization (Mott transition) across temperatures. Ionization behavior in this crossover region remains debated, with suggestions of a possible plasma-phase transition and competing state of fully and partially ionized hydrogen.[20] In Fig. 3(b), we compare the ionization degree at $r_{\rm WS} = 2$ with predictions from the neutral-pseudoatom (NPA) model[19,68] and the chemical-picture (CM) model proposed by Bellenbaum *et al.*.[29,35] For electron degeneracy parameters $\theta = 0.25$, 0.5, and 1, the NPA model predicts full ionization, whereas the CM model indicates partial ionization. Our calculations show that the plasmas are essentially fully ionized under these conditions. These pronounced differences between established models highlight the need for a more fundamental understanding of ionization equilibrium and plasma effects. For further insight, we compute the corresponding SFs for the uniform electron gas and for the hydrogen plasma at $r_{\rm WS} = 2$, $\theta = 1$, as displayed in Fig. 3(c). For the uniform electron gas, our model reproduces the PIMC reference data[28] with excellent accuracy. For the hydrogen plasma, a systematic deviation appears at wave numbers $k \lesssim 3$. This discrepancy may stem from approximations intrinsic to Chihara's treatment for the SFs,[60,61] which does not satisfy the compressibility sum rule for two-component plasmas.[69] However, this discrepancy does not significantly affect the integrated quantities such as IPD and EOS, since its influence is mitigated by the effect of electron screening.

In summary, we have developed a unified theoretical framework that self-consistently connects the ionization balance, EOS, and static SFs of matters. Our model clarifies the complex plasma effects governing ionization, incorporating thermal kinetic bottlenecks and pressure

ionization through a modified PF, and treating IPD through SFs to capture strong coupling physics. This approach naturally describes the smooth bound-continuum transition and elucidates the competing roles of thermal and pressure ionization. The framework reconciles contradictory predictions for ionization degree, and accurately reproduces high-fidelity PIMC EOS across a broad parameter range. By connecting microscopic electronic states to macroscopic thermodynamics, this work establishes a transferable and predictive foundation for modeling ionization and thermodynamics in partially ionized plasmas, with direct implications for high-energy-density experiments and astrophysical diagnostics.

Acknowledgments. This work was supported by the Science Challenge Project (Grant No. TZ2025013) and the National Natural Science Foundation of China (Grant Nos. 12474277, U2430208, and 12274384).

References

[1] Riffert H, Müther H, Herold H, and Ruder H 1996 *Matter at High Densities in Astrophysics* (Springer)
[2] Pradhan A K and Nahar S N 2011 *Atomic Astrophysics and Spectroscopy* (Cambridge University Press)
[3] Kraus D, Vorberger J, Pak A, Hartley N J, Fletcher L B, Frydrych S, Galtier E, Gamboa E J, Gericke D O, Glenzer S H, Granados E, MacDonald M J, MacKinnon A J, McBride E E, Nam I, Neumayer P, Roth M, Saunders A M, Schuster A K, Sun P, van Driel T, Döppner T, and Falcone R W 2017 *Nat. Astron.* **1** 606
[4] Hurricane O A, Patel P K, Betti R, Froula D H, Regan S P, Slutz S A, Gomez M R, and Sweeney M A 2023 *Rev. Mod. Phys.* **95** 025005
[5] Atzeni S and Meyer-Ter-Vehn J 2004 *The Physics of Inertial Fusion* (Oxford University Press)
[6] Faussurier G and Blancard C 2016 *Phys. Rev. E* **94** 033210
[7] Drake R P 2018 *High-Energy-Density Physics* (Springer)
[8] Kraus D, Preston T R, and Zastrau U 2026 *Nat. Rev. Phys.* **8** 27
[9] Chabrier G and Schatzman E (eds.) 1994 *The Equation of State in Astrophysics* (Cambridge University Press)
[10] Benedict L X, Driver K P, Hamel S, Militzer B, Qi T, Correa A A, Saul A, and Schwegler E 2014 *Phys. Rev. B* **89** 224109
[11] Döppner T, Swift D C, Kritcher A L, Bachmann B, Collins G W, Chapman D A, Hawreliak J, Kraus D, Nilsen J, Rothman S, Benedict L X, Dewald E, Fratanduono D E, Gaffney J A, Glenzer S H, Hamel S, Landen O L, Lee H J, LePape S, Ma T, MacDonald M J, MacPhee A G, Milathianaki D, Millot M, Neumayer P, Sterne P A, Tommasini R, and Falcone R W 2018 *Phys. Rev. Lett.* **121** 025001
[12] Zeng J, Huang Y, Deng A, Gao C, Hou Y, and Yuan J 2025 *Astron. Astrophys.* **698** A218
[13] Serenelli A M, Basu S, Ferguson J W, and Asplund M 2009 *Astrophys. J.* **705** L123
[14] Huebner W F and Barfield W D 2014 *Opacity* (Springer)
[15] Stanton L G and Murillo M S 2016 *Phys. Rev. E* **93** 043203
[16] Hou Y, Jin Y, Zhang P, Kang D, Gao C, Redmer R, and Yuan J 2021 *Matter Radiat. Extremes* **6** 026901
[17] Stanek L J, Kononov A, Hansen S B, Haines B M, Hu S X, Knapp P F, Murillo M S, Stanton L G, Whitley H D, Baalrud S D, Babati L J, Baczewski A D, Bethkenhagen M, Blanchet A, Clay Raymond C I, Cochrane K R, Collins L A, Dumi A, Faussurier G, French M, Johnson Z A, Karasiev V V, Kumar S, Lentz M K, Melton C A, Nichols K A, Petrov G M, Recoules V, Redmer R, Röpke G, Schörner M, Shaffer N R, Sharma V, Silvestri L G, Soubiran F, Suryanarayana P, Tacu M, Townsend J P, and White A J 2024 *Phys. Plasmas* **31** 052104
[18] Wetta N and Pain J C 2023 *Phys. Rev. E* **108** 015205
[19] Dharma-wardana M W C, Klug D D, Poole H, and Gregori G 2025 *Phys. Rev. E* **111** 015205
[20] Dharma-wardana M W C 2025 *Contrib. Plasma Phys.* e70072
[21] Ecker G and Kröll W 1966 *Z. Naturforsch. A* **21** 2023
[22] Gündel H 1970 *Beitr. Plasmaphys.* **10** 455
[23] Dharma-wardana M W C and Perrot F 1992 *Phys. Rev. A* **45** 5883
[24] Bethkenhagen M, Witte B B L, Schörner M, Röpke G, Döppner T, Kraus D, Glenzer S H, Sterne P A, and Redmer R 2020 *Phys. Rev. Res.* **2** 023260
[25] Wetta N and Pain J C 2025 *Contrib. Plasma Phys.* **65** e202500005
[26] Hu S X, Militzer B, Goncharov V N, and Skupsky S 2011 *Phys. Rev. B* **84** 224109
[27] Filinov A V and Bonitz M 2023 *Phys. Rev. E* **108** 055212
[28] Dornheim T, Schwalbe S, Böhme M P, Moldabekov Z A, Vorberger J, and Tolias P 2024 *J. Chem. Phys.* **160** 164111
[29] Moldabekov Z A, Shao X, Bellenbaum H M, Ma C, Mi W, Schwalbe S, Vorberger J, and Dornheim T 2025 *Matter Radiat. Extremes* **11** 025401
[30] Bethkenhagen M, Sharma A, Suryanarayana P, Pask J E, Sadigh B, and Hamel S 2023 *Phys. Rev. E* **107** 015306
[31] Plummer D, Svensson P, Gericke D O, Hollebon P, Vinko S M, and Gregori G 2025 *Phys. Rev. E* **111** 015204
[32] Demyanov G S and Levashov P R 2025 *Phys. Plasmas* **32** 123901
[33] Plummer D, Svensson P, Jasniak W, Hollebon P, Vinko S M, and Gregori G 2026 *Phys. Rev. E* **113** 045206
[34] Bonitz M and Kordts L 2025 *Contrib. Plasma Phys.* **65** e70001
[35] Bellenbaum H M, Böhme M P, Bonitz M, Döppner T, Fletcher L B, Gawne T, Kraus D, Moldabekov Z A, Schwalbe S, Vorberger J, and Dornheim T 2025 *Phys. Rev. Res.* **7** 033016
[36] Dharma-wardana M W C, Klug D D, and Remsing R C 2020 *Phys. Rev. Lett.* **125** 075702
[37] Bonitz M, Vorberger J, Bethkenhagen M, Böhme M P, Ceperley D M, Filinov A, Gawne T, Graziani F, Gregori G, Hamann P, Hansen S B, Holzmann M, Hu S X, Kählert H, Karasiev V V, Kleinschmidt U, Kordts L, Makait C, Militzer B, Moldabekov Z A, Pierleoni C, Preising M, Ramakrishna K, Redmer R, Schwalbe S, Svensson P, and Dornheim T 2024 *Phys. Plasmas* **31** 110501
[38] Stewart J C and Pyatt K D 1966 *Astrophys. J.* **144** 1203
[39] Wu C, Zhou F, Yan J, Gao X, Wu Y, Zeng C, and Wang J 2024 *Chin. Phys. Lett.* **41** 085202
[40] Zan X, Lin C, Hou Y, and Yuan J 2021 *Phys. Rev. E* **104** 025203
[41] Luo Q, Liang X, Lin C, Zhang X, Liu J, Gao C, Hou Y, and Yuan J 2025 *Phys. Rev. E* **111** 035208
[42] Röpke G, Blaschke D, Döppner T, Lin C, Kraeft W D, Redmer R, and Reinholz H 2019 *Phys. Rev. E* **99** 033201
[43] Hummer D G and Miralas D 1988 *Astrophys. J.* **331** 794
[44] Zaghloul M R 2010 *Phys. Plasmas* **17** 122903
[45] Kremp D, Schlanges M, and Kraeft W D 2005 *Quantum Statistics of Nonideal Plasmas* (Springer)
[46] Ebeling W 2017 *Contrib. Plasma Phys.* **57** 441
[47] Zaghloul M R 2013 *Phys. Lett. A* **377** 1119
[48] Shimamura I and Fujimoto T 1990 *Phys. Rev. A* **42** 2346
[49] Busquet M 2013 *High Energy Density Phys.* **9** 535
[50] Ebeling W 1974 *Physica* **73** 573
[51] Ebeling W and Sändig R 1973 *Ann. Phys.* **483** 289
[52] Lin C 2019 *Phys. Plasmas* **26** 122707
[53] Potekhin A Y 2010 *Phys. Plasmas* **17** 124705

[54] Hou Y, Jin F, and Yuan J 2007 *J. Phys.: Condens. Matter* **19** 425204
[55] Ebeling W, Kraeft W D, Kremp D, and Roepke G 1985 *Astrophys. J.* **290** 24
[56] Rogers F J 1986 *Astrophys. J.* **310** 723
[57] Zimmerman G and More R 1980 *J. Quant. Spectrosc. Radiat. Transfer* **23** 517
[58] Kawamura T, Mima K, and Koike F 1999 *Phys. Plasmas* **6** 3658
[59] Tsakiris G D and Eidmann K 1987 *J. Quant. Spectrosc. Radiat. Transfer* **38** 353
[60] Lin C, Röpke G, Kraeft W D, and Reinholz H 2017 *Phys. Rev. E* **96** 013202
[61] Chihara J 2000 *J. Phys.: Condens. Matter* **12** 231
[62] Gregori G, Ravasio A, Höll A, Glenzer S, and Rose S 2007 *High Energy Density Phys.* **3** 99
[63] Palmer R G and Weeks J D 1973 *J. Chem. Phys.* **58** 4171
[64] Singh H B and Holz A 1983 *Phys. Rev. A* **28** 1108
[65] Gericke D O, Vorberger J, Wünsch K, and Gregori G 2010 *Phys. Rev. E* **81** 065401
[66] Lin C, Hou Y, Yuan J, Wu Y, and Wang J 2026 *Plasma Phys. Control. Fusion* **68** 045042
[67] Pohl T, Vrinceanu D, and Sadeghpour H R 2008 *Phys. Rev. Lett.* **100** 223201
[68] Dharma-wardana M W C and Perrot F 1982 *Phys. Rev. A* **26** 2096
[69] Dharma-wardana M W C and Klug D D 2025 *Phys. Rev. E* **111** 065208